Published in final edited form as:

Cytoskeleton (Hoboken). 2015 July ; 72(7): 340–348. doi:10.1002/cm.21234.

TPX2 regulates neuronal morphology through kinesin-5 interaction

Olga I. Kahn[*], **Ngoc Ha**[*], **Michelle A. Baird**[†], **Michael W. Davidson**[†], and **Peter W. Baas**[*,‡]

[*]Department of Neurobiology and Anatomy, Drexel University College of Medicine, 2900 Queen Lane, Philadelphia, PA 19129, USA

[†]National High Magnetic Field Laboratory and Department of Biological Science, Florida State University, 1800 East Paul Dirac Drive, Tallahassee, Florida 32310, USA

Abstract

TPX2 (targeting protein for Xklp2) is a multifunctional mitotic spindle assembly factor that in mammalian cells localizes and regulates mitotic motor protein kinesin-5 (also called Eg5 or kif11). We previously showed that upon depletion or inhibition of kinesin-5 in cultured neurons, microtubule movements increase, resulting in faster growing axons and thinner dendrites. Here, we show that depletion of TPX2 from cultured neurons speeds their rate of process outgrowth, similarly to kinesin-5 inhibition. The phenotype is rescued by TPX2 re-expression, but not if TPX2's kinesin-5-interacting domain is deleted. These results, together with studies showing a spike in TPX2 expression during dendritic differentiation, suggest that the levels and distribution of TPX2 are likely to be determinants of when and where kinesin-5 acts in neurons.

Keywords

TPX2; neuron; molecular motor; microtubule; Eg5; kif11

Introduction

TPX2 was first discovered and named for its role in targeting Xklp2 (kinesin-12) during mitosis (Wittmann et al., 1998; Wittmann et al., 2000). Since its discovery, TPX2 has been shown to play numerous roles in cells, both in the nucleus and cytoplasm. During cell division, TPX2 imposes control over Aurora A kinase and mediates the accumulation of signaling and effector proteins on damaged chromatin in order to trigger and maintain cell cycle checkpoints, mediate DNA repair, or eliminate insulted cells (Brunet et al., 2004; Gruss et al., 2001; Kosodo et al., 2011; Kufer et al., 2002; Neumayer et al., 2012; Zorba et al., 2014). TPX2 is best known for its roles in influencing microtubules during mitosis. It regulates Ran-GTP-dependent microtubule assembly, bundles and organizes microtubules, interacts with the centrosome, and modulates the activity of kinesin-12 molecular motor protein.

[‡]Corresponding author: Baas PW, Ph.D., Department of Neurobiology and Anatomy, Drexel University College of Medicine, 2900 Queen Lane, Philadelphia, PA 19129 USA, Phone: 215-991-8298, Fax: 215-843-9082, pbaas@drexelmed.edu.

Conflict of interest: Authors declare no conflict of interest

Recently, TPX2 was shown to interact with kinesin-5 (also called Eg5 or kif11) at spindle microtubules for proper organization and functioning of those microtubules (Ma et al., 2010; Ma et al., 2011). Kinesin-5 is a slow homotetrameric motor with some overlap in properties and functions with kinesin-12 (Ferenz et al., 2010). In mitosis, kinesin-5 slowly slides apart anti-parallel microtubules to drive apart the bipolar spindle, while at the same time limits the rate at which microtubules are being slid by other motors. This effect has been likened to a brake on microtubule sliding imposed by kinesin-5, but the brake is energy-burning (not static as a crosslinker) as its slow motion overpowers the forces of other motors. In ways that are not as well understood, kinesin-5 can also interact with microtubules of the same polarity orientation, potentially also attenuating their motion by other motors. TPX2 binds not only to kinesin-5, but also to the microtubules with which kinesin-5 interacts, creating a drag on kinesin-5's motor activity (Leslie, 2011). In this way, kinesin-5's slow movement is further slowed effectively to non-motion, making it a true brake.

Kinesin-5 is re-purposed to play non-mitotic roles in terminally post-mitotic neurons (Ferhat et al., 1998), and so is TPX2 (Mori et al., 2009; Neumayer et al., 2012). We have found that treatment of cultured neurons with allosteric inhibitors of kinesin-5 or depletion of kinesin-5 with siRNA results in axons that grow faster (Myers and Baas, 2007) and fail to turn in response to guidance cues (Nadar et al., 2008; Nadar et al., 2012). Most recently, we reported that dendritic morphology is also affected by kinesin-5 inhibition, with dendrites of cultured rat sympathetic neurons mainly becoming thinner, but also shorter at one phase of their development (Kahn et al., 2015). Despite the fact that microtubules are organized quite differently in axons, dendrites, and growth cones, all of our observations to date best fit a model in which kinesin-5 acts as a brake to attenuate microtubule movements by other motor proteins. Much of the kinesin-5 in neurons is phosphorylated at a site required for it to interact with microtubules (Kahn et al., 2015), but it seems unlikely that phosphorylation at this site is the only means for regulating kinesin-5's activity. Here, we endeavored to test whether TPX2 is a regulator of kinesin-5's activity in neurons and potentially necessary in these cells as it appears to be during mitosis for kinesin-5 to act as a microtubule brake.

Results and Discussion

TPX2 expression in SCG neurons

TPX2 binds kinesin-5 through its C-terminal last 35 amino acids. Through its opposite end, TPX2 directly interacts with the same microtubules as the kinesin-5 homotetramer (Ma et al., 2010). In this manner, TPX2 creates a drag on the motor, which has been posited to be the means by which an already slow motor can be further slowed such that it behaves like an energy-burning brake on microtubule movements (Leslie, 2011). We wondered if in neurons kinesin-5 without TPX2 would not be sufficiently slow or sufficiently linked to the microtubules to behave in a brake-like fashion. TPX2 is typically confined to the nucleus in interphase cells, but two published studies have shown that it exists in the cytoplasm as well as the nucleus of cortical and dorsal root ganglion neurons (Mori et al., 2009; Neumayer et al., 2012). We first endeavored to ascertain its levels and distribution in superior cervical ganglion (SCG) neurons, using a commercial TPX2 antibody.

We confirmed the specificity of the antibody using rat RFL-6 fibroblasts, which were assayed 24 h after transfection with either control or TPX2 siRNA. A robust band at the appropriate molecular weight of 86 kDa for TPX2 was revealed on Western blots in the case of the control siRNA, with this band diminishing in the case of TPX2 siRNA. A similar reduction was obtained with SCG neurons that had been transfected with the siRNA for 48 h (Figure 1A). Western Blot analyses at different days *in vitro* (DIV) indicate that TPX2 expression in these neurons peaks during early dendrite development at around 6 DIV (Figure 1B), which follows the developmental distribution of kinesin-5 (Kahn et al., 2015). We previously found that the phosphorylated (the active, microtubule-associated) form of kinesin-5 (kinesin-5-pThr926) is concentrated at roughly twice the levels in dendrites compared to axons (Kahn et al., 2015). If TPX2 were required for kinesin-5 to act, we would expect TPX2 to be similarly enriched in dendrites relative to axons. To investigate this, we used a quantitative immunofluorescence approach. Neurons were grown for 6 DIV on PDL/Matrigel-coated glass coverslips (conditions that promote dendritic differentiation (Kahn et al., 2015), fixed and stained for TPX2 and MAP2 (a dendrite marker). TPX2 fluorescence intensity was measured within dendrites and axons and means of ratios of dendritic over axonal values were graphed (Figure 1C and D). We found that TPX2 is concentrated in dendrites compared to axons at 6 DIV similarly to kinesin-5-pThr926. We have long suspected that a defining difference between axons and dendrites may be far less mobility of microtubules in dendrites than in axons, but have never been able to show this due to technical limitations in live-imaging of microtubule transport in dendrites. If this is the case, kinesin-5 and TPX2 may play a central role in immobilizing microtubules in dendrites.

Kinesin-5's effects on neurite outgrowth are dependent upon TPX2

We wished to determine whether kinesin-5's activity in neurons is dependent upon TPX2. This is potentially complicated as TPX2 is known to be a multifunctional protein in mitotic cells and the same is true in neurons, where TPX2 has already been ascribed various functions (Mori et al., 2009; Neumayer et al., 2012). This would make prolonged depletion studies (needed for dendrites) difficult to interpret, as the various functions of TPX2 would make for a muddled interpretation of the phenotype. For this reason, we focused this portion of our studies on early process outgrowth with laminin. SCG neurons grow early processes very rapidly in the presence of laminin (more so than any other type of neuron that we have studied) and their rate of outgrowth is speeded even more by kinesin-5 depletion. This makes laminin-based process outgrowth from SCG neurons a rapid and sensitive readout of kinesin-5 activity, which we reasoned might enable us to dissect whether TPX2 is needed for kinesin-5's activity without the results being obstructed by other potential functions of TPX2 in neurons. We introduced control, TPX2 or kinesin-5 siRNA into SCG neurons by nucleofection at the time of plating (Figure 2). The neurons were re-plated after 48 h in order to visualize the effects of TPX2 depletion on process outgrowth over the next 6 h. For additional mechanistic insights, we added Monastrol or DMSO control to the cultures at the time of re-plating. Cultures were then fixed and stained for β3-tubulin (Figure 2A). Although all processes that grow from SCG neurons are generally considered to be axons until dendrites later appear in the cultures, we used the term "neurite" for the early processes that grew from the neurons under these experimental conditions. Measurements were made of total neurite length per neuron (Figure 2B and C). Without Monastrol present, both

TPX2-depleted and kinesin-5-depleted neurons displayed a statistically significant increase in neurite length relative to control siRNA. There was no significant difference between the TPX2-depleted and kinesin-5-depleted groups. We reasoned that if TPX2 depletion is causing neurites to grow longer because TPX2 is critical for kinesin-5 to act, then rendering kinesin-5 inactive through Monastrol treatment simultaneously with depleting TPX2 should not make processes grow any longer than depleting TPX2 alone. However, if other functions of TPX2 are at play (such as its interaction with other partner proteins or participation in other signaling pathways), the additive effect of kinesin-5 inhibition should make the neurites significantly longer than TPX2 depletion alone. We found that Monastrol treatment together with TPX2 depletion resulted in neurites that were no longer than either one alone (Figure 2C), which suggests that the greater neurite length observed with TPX2 depletion is due to TPX2's role in regulating kinesin-5's activity.

Effect of TPX2 overexpression in neurons

A great deal is known about how TPX2 interacts with microtubules (as well as kinesins-5 and 12) during mitosis. However, in typical interphase cells, TPX2 is restricted to the nucleus, as a result of nuclear localization signals within its sequence. We found that when we ectopically expressed a full-length wild-type (human) TPX2 construct in neurons, the entirety of the visible GFP-fusion protein appeared in the nucleus. Thus in order to mimic the endogenous protein's cytoplasmic distribution, we conducted site-directed mutagenesis to disable the nuclear localization signals (see Materials and Methods). In addition, we wished to make DNA constructs of TPX2 that would enable us to test its relevance to kinesin-5, which is possible to do because the domain of TPX2 that interacts with kinesin-5 is known. As indicated above, this domain consists of the C-terminal last 35 amino acids of the TPX2 protein (Ma et al., 2011). We generated three novel constructs of TPX2: C-terminal 35 amino acids, which we called mEmerald-35TPX2; a full-length construct with necessary nuclear localization sequence mutations for the construct to localize outside of the nucleus, which we called mEmerald-fullTPX2; and a slightly shorter construct with necessary nuclear localization sequence mutations for the construct to be localized outside of the nucleus but without the kinesin-5 interacting domain, which we called mEmerald-shortTPX2 (Figure 3A). A peptide corresponding to the kinesin-5 binding domain has previously been microinjected into cells, wherein it performed reliably to specifically inhibit TPX2's ability to interact with kinesin-5 (Ma et al., 2011).

In order to determine the effects of these constructs on neuronal morphology, we expressed them in neurons (alongside mEmerald control) for 24 h (Figure 3B). We reasoned that if the phenotype we observed with TPX2 depletion is due primarily to its importance in the braking ability of kinesin-5, expression of the mEmerald-35TPX2 should produce an effect similar to depletion of TPX2, namely longer neurites. Available TPX2-binding sites on kinesin-5 would be occupied by mEmerald-35TPX2, thus inhibiting the endogenous TPX2 from interacting with the motor. Indeed, neurites of neurons expressing this construct were significantly longer than neurites of neurons expressing the control mEmerald construct (Figure 3C and D). We predicted that neurons expressing the mEmerald-fullTPX2 would have shorter neurites than controls, since more of the kinesin-5 motors would be interacting with TPX2 and because TPX2 has its own microtubule-bundling properties irrespective of

kinesin-5 (Schatz et al., 2003; Kosodo et al., 2011). This prediction was born out. We also found that expressing mEmerald-shortTPX2 results in significantly shorter neurites than control neurons, which is expected on the basis of TPX2's microtubule-bundling properties.

TPX2 requires kinesin-5 binding-domain to rescue neurite growth phenotype

TPX2 is a complicated protein that interacts with a number of other proteins (Brunet et al., 2004; Giubettini et al., 2011; Ma et al., 2011; Wittmann et al., 2000). Therefore, we wished to conduct additional studies to confirm TPX2's relevance to kinesin-5's activity in neurons. In theory, if our observed TPX2 knockdown phenotype on process outgrowth is dependent upon TPX2's interaction with kinesin-5, mEmerald-fullTPX2 should rescue the phenotype but mEmerald-shortTPX2 should not. To test this, SCG neurons were cultured and treated with control or TPX2 siRNA at the time of plating. After 2 DIV, the neurons were re-plated onto glass coverslip dishes and after 1 h electroporated via Cellaxess with control mEmerald, mEmerald-fullTPX2 or mEmerald-shortTPX2 constructs. In this manner, the endogenous TPX2 was depleted by the time the constructs were introduced and expressed for the next 24 h. For these experiments, we selected neurons with somewhat lower expression levels of the TPX2 constructs to avoid diminution in process outgrowth as a result of TPX2's own microtubule-bundling properties (Figure 4A). After growing for 24 h post transfection, both full-length and short TPX2 construct expression yielded neurites that were not significantly shorter than control (Figure 4B). In the TPX2-depleted neurons, expression of mEmerald-fullTPX2 rescued the TPX2 depletion neurite length phenotype by significantly reducing it, while neurite length in neurons expressing the mEmerald-shortTPX2 was not significantly different from mEmerald-control (Figure 4B and D). These results indicate that the kinesin-5-binding domain of TPX2 is necessary for it to rescue the observed phenotype. Figure 4C schematically shows the logic of the experiment.

Kinesin-5 requires TPX2 as a microtubule brake in neurons

A challenge for the present studies was to design experiments in a manner that could be interpreted in terms of kinesin-5 function, as TPX2 has been reported in neurons to participate in signaling pathways in neurons that are not known to involve kinesin-5 (Mori et al., 2009). In developing cortical and dorsal root ganglion neurons, TPX2 has been found to cooperate with Aurora A, Ndel1, and the atypical protein kinase C to remodel microtubules at the neurite hillock. Interference of this pathway in previous studies caused a significant decrease in the frequency of microtubules emanating from the centrosome, resulting in impaired neurite extension (Mori et al., 2009; Neumayer et al., 2014). Whether or not this pathway exists in SCG neurons is unknown. However, SCG neurons have the technical advantage for our present studies of immediate and rapid neurite outgrowth on laminin, which we found to be augmented by TPX2 depletion. Our results indicate that this effect is due to a requisite role for TPX2 in the microtubule-related functions of kinesin-5 in neurons. A different mode of neurite outgrowth may be sensitive to TPX2's involvement in other pathways, such as the one studied by the previous authors.

We previously reported that depletion or inhibition of kinesin-5 in developing neurons has notable effects on axonal growth, branching and navigation, as well as dendritic shape. Mechanistically, our previous studies showed that kinesin-5 limits movements of

microtubules that would otherwise occur via other molecular motors, such as cytoplasmic dynein or kinesin-6 (Myers and Baas, 2007; Nadar et al., 2008; Lin et al., 2012). One of the greatest puzzles about kinesin-5 is how a motor protein that should generate motion acts to oppose motion. Given that kinesin-5 is a very slow motor, about 100 times slower than dynein (Kapitein et al., 2005; Paschal and Vallee, 1987), one idea is that its slow motion is tantamount to non-motion, which wins out in a competition with any other motor. But are kinesin-5's own properties sufficient for this effect? It has been speculated that the effects of kinesin-5 during mitosis require assistance from TPX2, which binds directly to kinesin-5 and also extends outward to bind to the same microtubules as the kinesin-5 homotetramer (Ma et al., 2011). Thus, as kinesin-5 generates its slow motion, TPX2 creates a drag on the motion, slowing it further. In this way, kinesin-5's activity is energy-dependent, but is fortified by interactions with the relevant microtubules by TPX2 (see Introduction). Our present results suggest that this is the case in neurons, as depletion of TPX2 generates the same phenotype as depletion of kinesin-5, and so too does expression of the kinesin-5 binding domain of TPX2, which acts as a dominant-negative to impede the normal interaction of the two endogenous proteins. This cross-linking function of TPX2 can also explain how kinesin-5 might impede microtubule movements in axons, where microtubules are almost exclusively of the same orientation, as well as dendrites, where microtubules are of mixed orientations (Baas et al., 1989; Kahn et al., 2015; Lin et al., 2012). Thus, we suggest that together, kinesin-5 and TPX2 act in neurons as a brake on microtubule-microtubule movements, both in the case of parallel and anti-parallel microtubules.

A brake, to be effective, must be adjustable and TPX2 interaction provides a level of regulation, in addition to those that we have previously reported (Kahn et al., 2015). Ascertaining what drives the two proteins to interact and whether this interaction is always in place in neurons will further shed light on cytoskeletal development of axons and dendrites. We posit that the partnership of kinesin-5 and TPX2 is especially important during development, because the microtubule-brake would be responsive to signaling cascades that can modulate axonal growth rates, navigation of the growth cone, speed and cessation of neuronal migration, and the shape of dendrites. In addition, TPX2 might provide a link between kinesin-5's activity and the numerous other pathways with which TPX2 interacts in developing neurons. Such mechanisms may also be important in adult neurons, and if so, there is relevance to potential side effects of drug therapies for cancer or nerve regeneration based on inhibitors of kinesin-5 or TPX2.

Materials and methods

Cell culture

Cultures of dissociated neurons from rat superior cervical ganglia (SCG) were prepared as previously described from P 1–2 pups of either sex (He et al., 2005) from timed-pregnant Sprague-Dawley rats purchased from Taconic. The neurons were cultured in L-15 medium (Gibco) supplemented with D(+)glucose (Sigma), GlutaMax-I (Gibco), Penn/Strep (Sigma), FBS (HyClone) and NGF (Upstate Biotech). The following day, 5 μM arabinose C (Calbiochem) was added to the medium to suppress proliferation of dividing (non-neuronal) cells. For longer-term cultures, at 3 DIV, to enhance dendritic differentiation, the medium

was replaced with F12/DMEM medium (Gibco) supplemented with BSA (Calbiochem), GlutaMax-I, N2 (Gibco), FBS and NGF. Neurons were plated on either plastic 35 mm dishes or dishes with a 1 cm hole covered by a glass coverslip (MatTek). All dishes were coated with 1 mg/mL poly-D-lysine (PDL) (Sigma) at +4°C overnight, washed extensively with water and then kept in water overnight at +37°C. For 24 h experiments neurons were plated directly on PDL coated glass coverslips. For re-plating experiments, the neurons were first plated on 35 mm plastic dishes. At 2 DIV, the neurons were dislodged with 0.25% trypsin (Gibco) and re-plated at a density of 7,000 cells per dish (for siRNA studies) or 15,000 cells per dish (for further transfection with DNA constructs) onto glass-bottomed dishes. Plating neurons at a greater density in the case of a high stress second electroporation of a construct improved their recovery and viability. After the cells had adhered to the glass, 30 min later, 2 mL L-15 plating medium were added together with 1:400 laminin (Sigma). Neurons were fixed after 6 h. For 24 h studies and beyond, no laminin was added. For studies on dendrites, neurons were plated directly after dissection and dissociation onto glass-bottomed dishes that had been coated with 1 mg/ml PDL followed by Matrigel (BD Bioscience) (for 3 h) to hasten dendritic development. Under these conditions *bona fide* dendrites developed by DIV 5–6. RFL-6 cells (rat fibroblast) were used to test efficacy of the TPX2 antibody. Cells were maintained in F12K medium supplemented with 10% FBS. Transfected cells were plated for 24 h on plastic dishes for Western Blot analysis. Control siRNA was purchased from Ambion, siRNA pools for rat kinesin-5 and rat TPX2 were purchased from Sigma-Aldrich. In the case of the latter, care was taken to ensure that the sequences did not affect human TPX2, so that rescue experiments could be performed with human TPX2 constructs.

Drug treatments

Monastrol (Calbiochem) was dissolved in DMSO (Sigma). DMSO alone was as the control for Monastrol experiments at 0.1% final concentration. Drug or DMSO was added with medium 30 min after plating, allowing neurons to settle, and cultures were fixed 6 h later.

Transfection

Amaxa nucleofector was used to introduce siRNA or constructs into cells at the time of plating (He et al., 2005). Cellaxess ACE (Cellectricon) device was used to transfect constructs at 10 μg/100 μL concentration into adherent neuronal cultures. ACE protocol used was 260 V, 2 ms long, 10 pulses with 1 s interval.

Antibodies

Rabbit polyclonal antibody against MAP2 was provided by Dr. Itzhak Fischer, Drexel University College of Medicine, Philadelphia, PA (Nunez and Fischer, 1997). Other antibodies were purchased as follows: β3-tubulin rabbit polyclonal and mouse monoclonal antibody (Covance), β-tubulin cy3 conjugated monoclonal mouse antibody (Sigma), TPX2 rabbit polyclonal antibody (Santa Cruz Biotechnology), mouse monoclonal actin antibody (Abcam), mouse monoclonal GAPDH antibody (Abcam). Appropriate fluorescent goat secondary antibodies were purchased from Jackson Immunoresearch.

Plasmids

The human TPX2 (NM_012112) expression vectors were constructed using a C1 (Clontech-style) cloning vector and an advanced EGFP variant, mEmerald (wtGFP + F64L, S65T, S72A, N149K, M153T, I167T, A206K). The TPX2 c-terminal fragment 35 (a.a. 713–747) was generated based on previous work (Ma et al., 2010). The following primers were used to amplify the TPX2 and produce a benign 18 amino acid linker (SGLRSRAQASGDSGGSGS) separating mEmerald from the TPX2 fragments. Fragment 35 (a.a. 713–747): (HindIII forward: AGT ATA AGC TTC GGG AGA TAG TGG TGG GAG CGG TTC ACA TAA GGC AAA TCC AAT ACG CAA GTA CCA GGG TCT GG) and (BamHI reverse: CGA CGA GGA TCC TTA GCA GTG GAA TCG AGT GGA GAA TTT GGG AGA TAC AGG C). The resulting PCR products and mEmerald-C1 cloning vector were digested with the appropriate restriction enzymes, gel purified, and ligated to yield mEmerald-TPX2-713-747-C-18. Full-length and short TPX2 constructs were generated in a similar fashion, however with several point mutations. We found that full-length un-mutated TPX2 would localize to the nucleus exclusively and so would a construct with the main NLS mutated [K313A, K314A, R315A in human sequence (Brunet et al., 2004)]. Therefore, we mutated K158A, K159A, K313A, K314A, R315A (Schatz et al., 2003; Vos et al., 2008) for cytoplasmic localization of mEmerald-TPX2-1-747-C-18 and mEmerald-TPX2-1-712-C-18. Empty mEmerald-C1 cloning vector was used as a control for experiments with these new TPX2 constructs.

Western blotting

Total protein from cultures of rat SCG neurons or RFL-6 cells was extracted using 1-to-1 sample buffer and CelLytic M (Sigma) from neurons plated on plastic 35 mm dishes coated with 1mg/mL PDL. Neurons were treated with arabinose C in order to minimize non-neuronal cells. The Bio-Rad Mini-PROTEAN Tetra Cell system was used for electrophoretic separation of the protein samples, according to manufacturer's instructions. Protein samples were resolved using 7.5% SDS-PAGE. The gel was transferred onto nitrocellulose membranes (Bio-Rad). The blots were blocked with 5% milk in TBST (BioRad, Fisher) and then probed with primary antibodies at +4°C overnight. After washing, the blots were incubated with peroxidase-conjugated secondary IgG. Membrane-bound peroxidase was visualized on Pierce CL-XPosure Film after treatment with ECL Western Blotting Substrate (Thermo Scientific). Levels of protein of interest were normalized with actin or GAPDH for each group and expressed as densitometric ratios against DIV 1 or control.

Quantitative fluorescence microscopy

Neurons were fixed with 4% paraformaldehyde and 0.2% glutaraldehyde simultaneously with extraction (0.2% Triton X-100) in PHEM buffer for 15 min and then washed extensively with PBS. Immunofluorescence staining was conducted as previously described (Liu et al., 2010). Primary antibodies were incubated overnight at +4°C and the secondary antibodies were applied the next day for 1 h at +37°C. All images were taken using an Axiovert 200 inverted microscope (Carl Zeiss) and image analysis was done using the Axiovision 4.6 software. Each cell was imaged with a 40x objective and images used for

quantification did not contain saturated pixels in axons or dendrites. All images within comparable groups were taken with appropriate rigor and under identical settings. Neurite length was measured from the base of the neurite to its visible end from β3-tubulin immunostained cultures. Average immunofluorescence intensity was measured within a box drawn over the region of interest (ROI) in the dendrite (the brightest part of the dendrite) and axon within the same image. Size of ROIs was kept consistent throughout the experiments; volume differences between axons and dendrites were corrected for. Background intensity was subtracted from all measurements.

Statistical analyses

All data analyses and statistical comparisons were performed using SPSS 23 (IBM). Graphs were generated using SPSS, Plotly and Excel (Microsoft). The outcome variables for neurite length exhibited a positively skewed distribution and were graphed in a histogram for each condition in the corresponding figures. Data were graphed using mean plus/minus standard error of the mean of at least 2 repeats for each experiment. For statistical analyses, the mean difference was considered to be significant at the 0.05 level ($p<0.05$*, $p<0.01$**, $p<0.001$***).

Presentation of images

Figures were processed with Adobe Photoshop CS2 and Illustrator CS2. In some cases, fluorescence images were brightened in order to show all neurites clearly only for presentation purposes – this was done for all conditions identically.

Acknowledgments

This work was supported by a grant to PWB from the National Institutes of Health. OIK is the recipient of a pre-doctoral NRSA fellowship from the National Institutes of Health.

References

Baas PW, Black MM, Banker GA. Changes in microtubule polarity orientation during the development of hippocampal neurons in culture. J Cell Biol. 1989; 109(6 Pt 1):3085–94. [PubMed: 2592416]

Brunet S, Sardon T, Zimmerman T, Wittmann T, Pepperkok R, Karsenti E, Vernos I. Characterization of the TPX2 domains involved in microtubule nucleation and spindle assembly in Xenopus egg extracts. Mol Biol Cell. 2004; 15(12):5318–28. [PubMed: 15385625]

Ferenz NP, Gable A, Wadsworth P. Mitotic functions of kinesin-5. Semin Cell Dev Biol. 2010; 21(3): 255–9. [PubMed: 20109572]

Ferhat L, Cook C, Chauviere M, Harper M, Kress M, Lyons GE, Baas PW. Expression of the mitotic motor protein Eg5 in postmitotic neurons: implications for neuronal development. J Neurosci. 1998; 18(19):7822–35. [PubMed: 9742151]

Giubettini M, Asteriti IA, Scrofani J, De Luca M, Lindon C, Lavia P, Guarguaglini G. Control of Aurora-A stability through interaction with TPX2. J Cell Sci. 2011; 124(Pt 1):113–22. [PubMed: 21147853]

Gruss OJ, Carazo-Salas RE, Schatz CA, Guarguaglini G, Kast J, Wilm M, Le Bot N, Vernos I, Karsenti E, Mattaj IW. Ran induces spindle assembly by reversing the inhibitory effect of importin alpha on TPX2 activity. Cell. 2001; 104(1):83–93. [PubMed: 11163242]

He Y, Francis F, Myers KA, Yu W, Black MM, Baas PW. Role of cytoplasmic dynein in the axonal transport of microtubules and neurofilaments. J Cell Biol. 2005; 168(5):697–703. [PubMed: 15728192]

Kahn OI, Sharma V, Gonzalez-Billault C, Baas PW. Effects of kinesin-5 inhibition on dendritic architecture and microtubule organization. Mol Biol Cell. 2015; 26(1):66–77. [PubMed: 25355946]

Kapitein LC, Peterman EJ, Kwok BH, Kim JH, Kapoor TM, Schmidt CF. The bipolar mitotic kinesin Eg5 moves on both microtubules that it crosslinks. Nature. 2005; 435(7038):114–8. [PubMed: 15875026]

Kosodo Y, Suetsugu T, Suda M, Mimori-Kiyosue Y, Toida K, Baba SA, Kimura A, Matsuzaki F. Regulation of interkinetic nuclear migration by cell cycle-coupled active and passive mechanisms in the developing brain. EMBO J. 2011; 30(9):1690–704. [PubMed: 21441895]

Kufer TA, Sillje HH, Korner R, Gruss OJ, Meraldi P, Nigg EA. Human TPX2 is required for targeting Aurora-A kinase to the spindle. J Cell Biol. 2002; 158(4):617–23. [PubMed: 12177045]

Leslie M. TPX2 is a drag on Eg5. J Cell Biol. 2011; (32):14033–14049.

Lin S, Liu M, Mozgova OI, Yu W, Baas PW. Mitotic motors coregulate microtubule patterns in axons and dendrites. J Neurosci. 2012; 32(40):14033–49. [PubMed: 23035110]

Liu M, Nadar VC, Kozielski F, Kozlowska M, Yu W, Baas PW. Kinesin-12, a mitotic microtubule-associated motor protein, impacts axonal growth, navigation, and branching. J Neurosci. 2010; 30(44):14896–906. [PubMed: 21048148]

Ma N, Titus J, Gable A, Ross JL, Wadsworth P. TPX2 regulates the localization and activity of Eg5 in the mammalian mitotic spindle. J Cell Biol. 2011; 195(1):87–98. [PubMed: 21969468]

Ma N, Tulu US, Ferenz NP, Fagerstrom C, Wilde A, Wadsworth P. Poleward transport of TPX2 in the mammalian mitotic spindle requires dynein, Eg5, and microtubule flux. Mol Biol Cell. 2010; 21(6):979–88. [PubMed: 20110350]

Mori D, Yamada M, Mimori-Kiyosue Y, Shirai Y, Suzuki A, Ohno S, Saya H, Wynshaw-Boris A, Hirotsune S. An essential role of the aPKC-Aurora A-NDEL1 pathway in neurite elongation by modulation of microtubule dynamics. Nat Cell Biol. 2009; 11(9):1057–68. [PubMed: 19668197]

Myers KA, Baas PW. Kinesin-5 regulates the growth of the axon by acting as a brake on its microtubule array. J Cell Biol. 2007; 178(6):1081–91. [PubMed: 17846176]

Nadar VC, Ketschek A, Myers KA, Gallo G, Baas PW. Kinesin-5 is essential for growth-cone turning. Curr Biol. 2008; 18(24):1972–7. [PubMed: 19084405]

Nadar VC, Lin S, Baas PW. Microtubule redistribution in growth cones elicited by focal inactivation of kinesin-5. J Neurosci. 2012; 32(17):5783–94. [PubMed: 22539840]

Neumayer G, Helfricht A, Shim SY, Le HT, Lundin C, Belzil C, Chansard M, Yu Y, Lees-Miller SP, Gruss OJ, et al. Targeting protein for xenopus kinesin-like protein 2 (TPX2) regulates gamma-histone 2AX (gamma-H2AX) levels upon ionizing radiation. J Biol Chem. 2012; 287(50):42206–22. [PubMed: 23045526]

Nunez J, Fischer I. Microtubule-associated proteins (MAPs) in the peripheral nervous system during development and regeneration. J Mol Neurosci. 1997; 8(3):207–22. [PubMed: 9297633]

Paschal BM, Vallee RB. Retrograde transport by the microtubule-associated protein MAP 1C. Nature. 1987; 330(6144):181–3. [PubMed: 3670402]

Schatz CA, Santarella R, Hoenger A, Karsenti E, Mattaj IW, Gruss OJ, Carazo-Salas RE. Importin alpha-regulated nucleation of microtubules by TPX2. EMBO J. 2003; 22(9):2060–70. [PubMed: 12727873]

Vos JW, Pieuchot L, Evrard JL, Janski N, Bergdoll M, de Ronde D, Perez LH, Sardon T, Vernos I, Schmit AC. The plant TPX2 protein regulates prospindle assembly before nuclear envelope breakdown. Plant Cell. 2008; 20(10):2783–97. [PubMed: 18941054]

Wittmann T, Boleti H, Antony C, Karsenti E, Vernos I. Localization of the kinesin-like protein Xklp2 to spindle poles requires a leucine zipper, a microtubule-associated protein, and dynein. J Cell Biol. 1998; 143(3):673–85. [PubMed: 9813089]

Wittmann T, Wilm M, Karsenti E, Vernos I. TPX2, A novel xenopus MAP involved in spindle pole organization. J Cell Biol. 2000; 149(7):1405–18. [PubMed: 10871281]

Zorba A, Buosi V, Kutter S, Kern N, Pontiggia F, Cho YJ, Kern D. Molecular mechanism of Aurora A kinase autophosphorylation and its allosteric activation by TPX2. Elife. 2014; 3:e02667. [PubMed: 24867643]

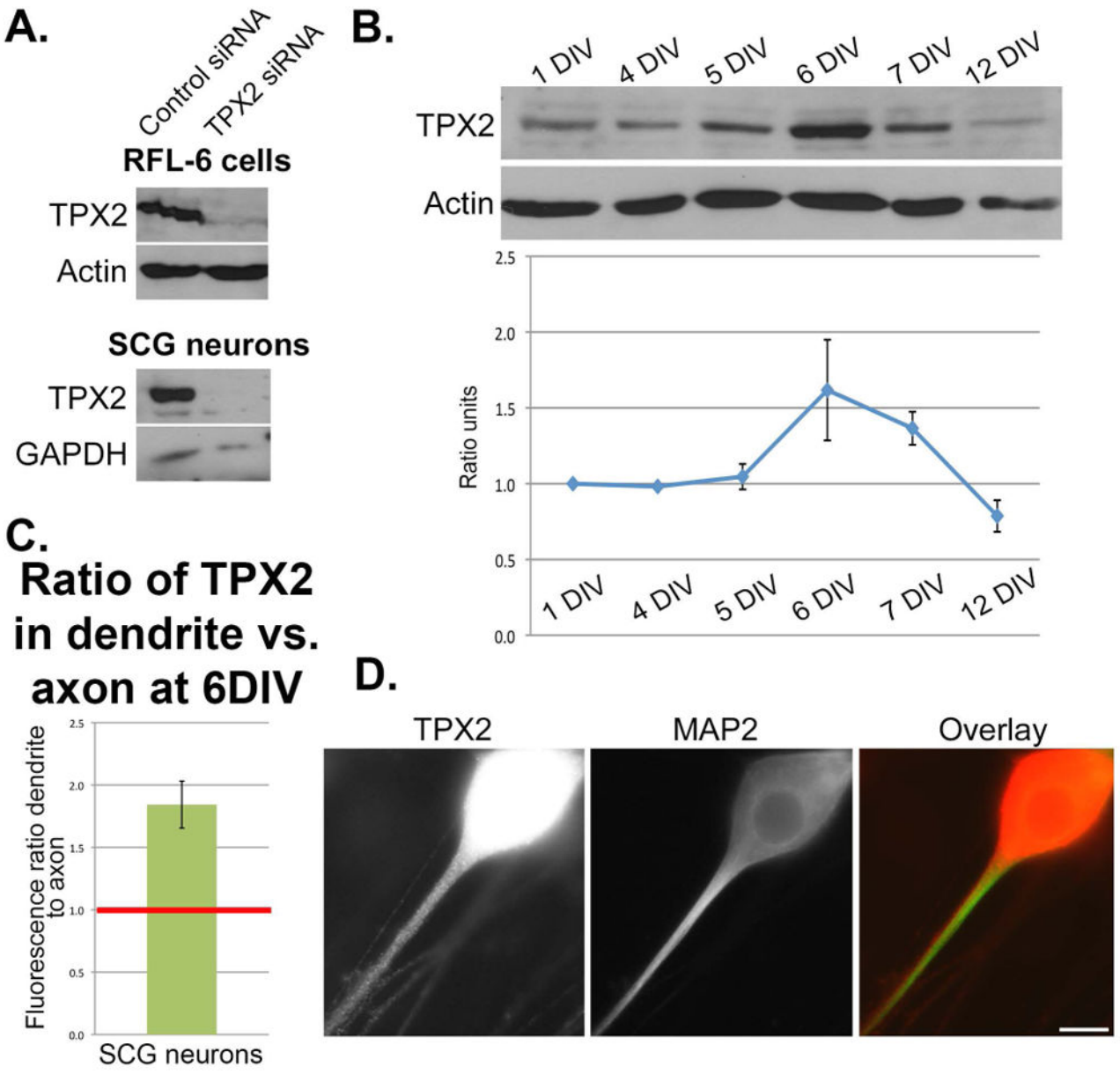

Figure 1. TPX2 expression in neurons

(**A**) TPX2 antibody is verified to recognize endogenous TPX2 in rat RFL-6 cells and rat SCG neurons. RFL-6 cells and SCG neurons were treated with control or TPX2 siRNA and collected for Western Blot respectively after 24h and 48h. The blot was probed for TPX2 and actin or GAPDH as internal control. (**B**) SCG neurons were plated and collected after 1, 4, 5, 6, 7 and 12 DIV. Samples were run on Western Blot and probed for TPX2 as well as for actin as internal control. Densitometric values were measured via ImageJ and normalized first against actin and then displayed as a ratio against 1 DIV. (**C**) SCG neurons were cultured for 6 DIV, fixed and stained for TPX2. Fluorescence was measured using the same sized rectangle within the proximal dendrite and a bundle of axons within the same image as determined by MAP2 dendrite marker. Background fluorescence was subtracted from all

measurements. A ratio of dendrite over axon fluorescence was normalized against β3-tubulin volume measurements: 1.84±(0.19)-to-1, n=28. (**D**) Representative images from quantifications in C are presented. TPX2 is red and MAP2 is green. Processes in the TPX2 image that do not stain for MAP2 are axons. Bar 10 μm.

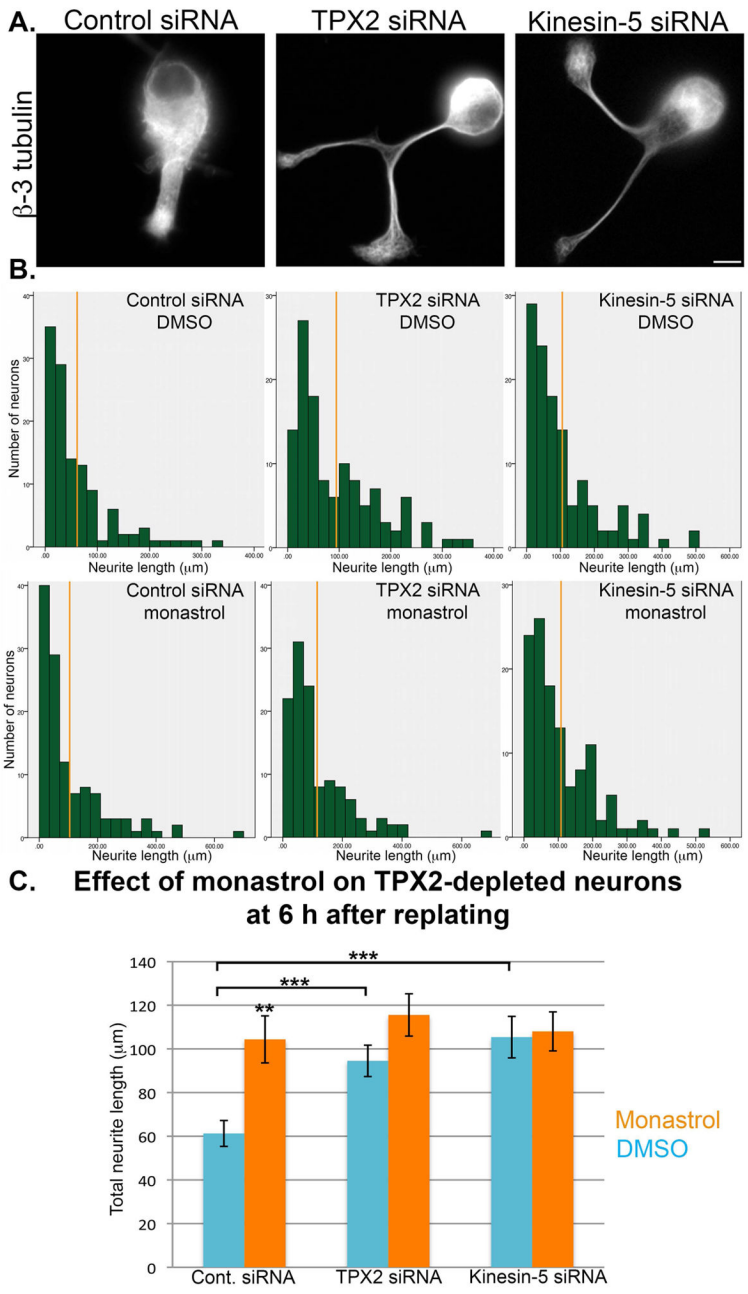

Figure 2. TPX2-depleted neurons grow neurites as fast as kinesin-5-depleted neurons

(**A**) Neurons were isolated from SCGs and transfected with control, TPX2 or kinesin-5 siRNA. At 3 DIV, neurons were re-plated from plastic dishes onto glass coverslip dishes and Monastrol or DMSO (as control) was added. Neurons were fixed after 6 h, stained against β3-tubulin and quantified for total neurite length. Bar is 10 μm. (**B**) Data for each condition were positively skewed and graphed into a histogram. X-axis are binned neurite lengths, y-axis is frequency. Orange line denotes the mean. (**C**) Mann-Whitney U test showed significant difference between control siRNA DMSO (median 34.73 μm; mean 61.27±5.93 μm; n=120) and control siRNA Monastrol groups (median 54.31 μm; mean 104.35±10.77

μm; n=120; U=5608.5, p>0.01). There was also a significant difference between control siRNA DMSO group and TPX2 siRNA DMSO (median 62.75 μm; mean 94.52±7.18 μm; n=120; U=4997.5, p>0.001) and Kinesin-5 DMSO groups (median 66.99 μm; mean 105.38±9.51 μm; n=120; U=5056.5, p>0.001). There was no significant difference between TPX2 siRNA DMSO and TPX2 siRNA Monastrol (median 81.77 μm; mean 115.54±9.69 μm; n=120; U=6364, p=0.12) and between kinesin-5 siRNA DMSO and kinesin-5 siRNA Monastrol (median 71.81 μm; mean 108.02±8.93 μm; n=120; U=6827, p=0.49).

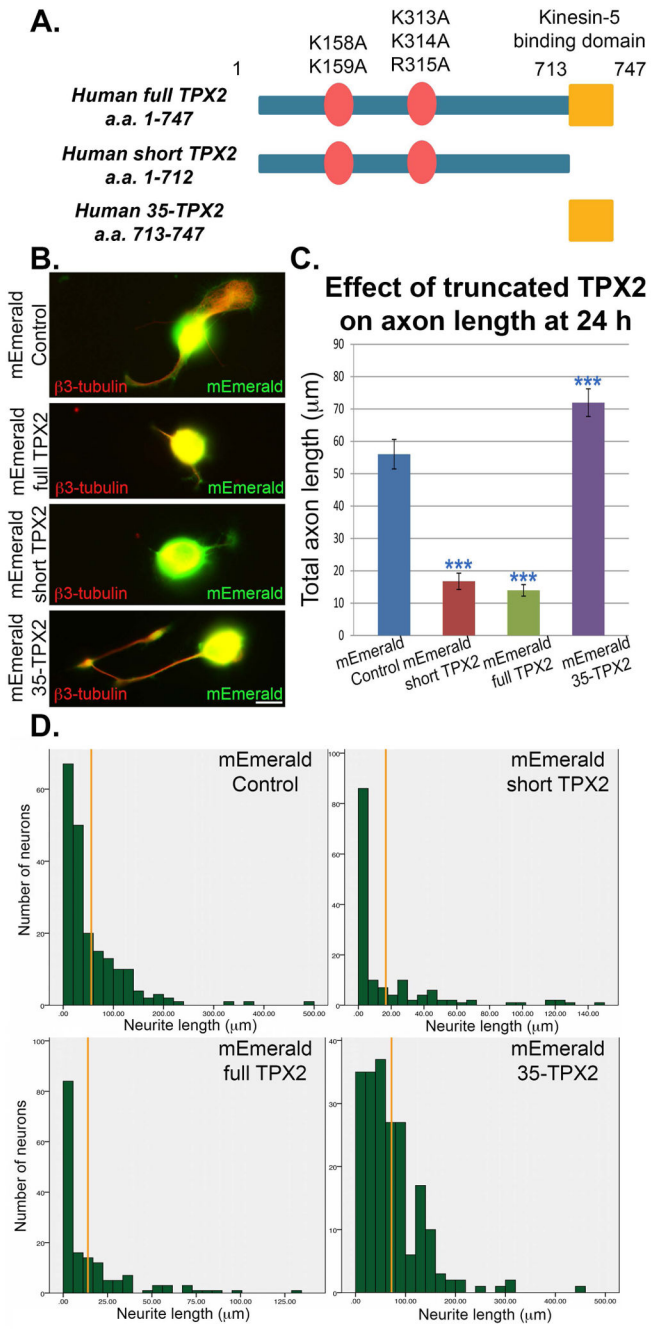

Figure 3. Effect of TPX2 constructs expression on neurons

(**A**) Full-length (mEmerald-fullTPX2), short (mEmerald-shortTPX2) and truncated (mEmerald-35TPX2) constructs were generated with the denoted modifications. (**B**) The three TPX2 constructs or control empty vector were individually introduced into SCG neurons via nucleofection at the time of plating. After 24 h, neurons were fixed and immunostained for β3-tubulin. Bar 10 μm. (**C**) Mann-Whitney U test showed significant difference between mEmerald control (median 31.61 μm; mean 56.03±4.56 μm; n=200) and mEmerald-shortTPX2 (median >1 μm; mean 16.76±2.52 μm; n=144; U=5341, p<0.001),

mEmerald-fullTPX2 (median 4.77 μm; mean 13.96±1.77 μm; n=158; U=5390, $p<0.001$) and mEmerald-35TPX2 (median 56.53 μm; mean 71.96±4.27 μm; n=206; U=15697.5, $p<0.001$) (**D**) Data for each condition were positively skewed and graphed into a histogram. X-axis are binned neurite lengths, y-axis is frequency. Orange line denotes the mean.

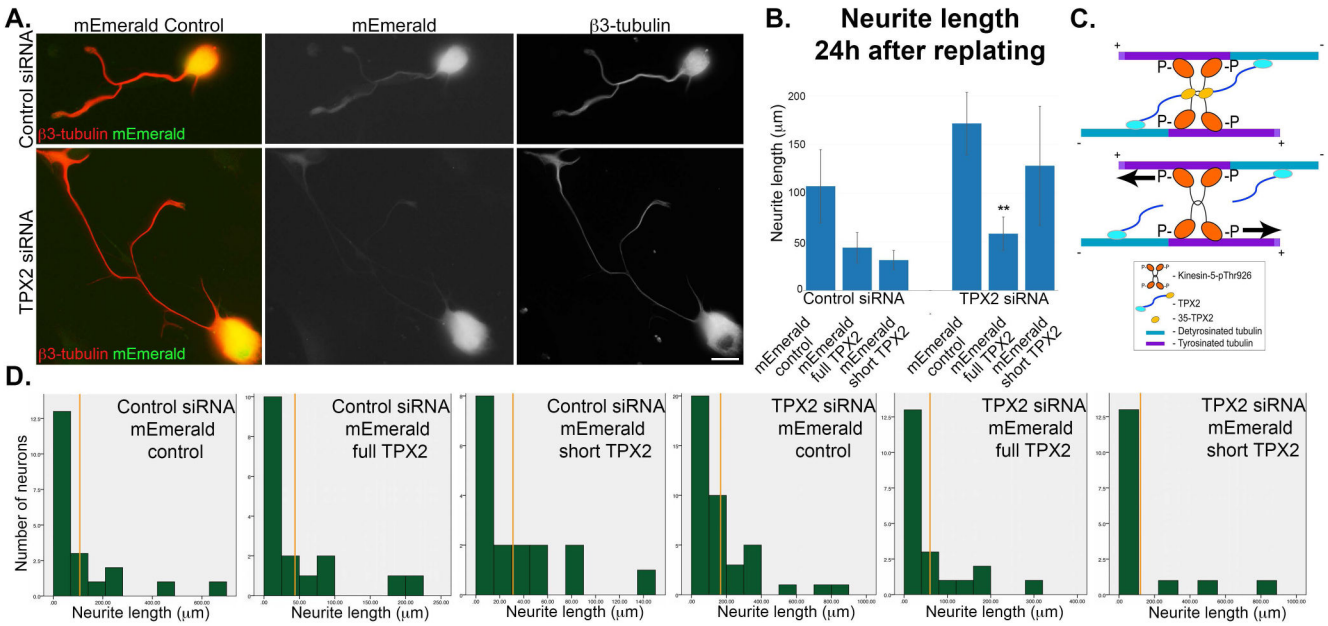

Figure 4. Neurite length of TPX2-depleted neurons cannot be rescued TPX2 lacking kinesin-5 interacting domain

(**A**) Control or TPX2 siRNA was introduced into SCG neurons via nucleofection at the time of plating. After 2 DIV, neurons were re-plated and transfected with mEmerald control, mEmerald-fullTPX2 or mEmerald-shortTPX2 constructs for 24 h. Cells stained for β3-tubulin and expressing the constructs were quantified for neurite length. Bar 10 μm. (**B**) Mann-Whitney U test showed no significant difference between control siRNA mEmerald control (median 29.78 μm; mean 106.93±37.59 μm; n=21) and control siRNA mEmerald-fullTPX2 (median 14.67 μm; mean 43.88±15.49 μm; n=17; U=137.5, p=0.23) and control siRNA mEmerald-shortTPX2 (median 21.11 μm; mean 31.07±9.90 μm; n=17; U=126, p=0.13). Mann-Whitney U test showed significant difference between TPX2 siRNA mEmerald control (median 104.41 μm; mean 167.21±31.47 μm; n=41) and TPX2 siRNA mEmerald-fullTPX2 (median 25.57 μm; mean 59.86±17.87 μm; n=21; U=272, p=0.02), but no significant difference with TPX2 siRNA mEmerald-shortTPX2 (median 26.17 μm; mean 121.46±57.60 μm; n=16; U=225, p=0.07) (**C**) Schematic of TPX2 interaction with kinesin-5 and their effects on microtubules. (**D**) Data for each condition were positively skewed and graphed into a histogram. X-axis are binned neurite lengths, y-axis is frequency. Orange line denotes the mean.